Program Digest, 2019 IEEE International Ultrasonics Symposium (IUS)
Glasgow, Scotland, October 6-9, 2019

An in-air ultrasonic acoustic beam shifter metamaterial

Paul Daly
Centre for Ultrasonic Engineering
University of Strathclyde
Glasgow, United Kingdom
paul.daly@strath.ac.uk

Prof James F.C. Windmill
Centre for Ultrasonic Engineering
University of Strathclyde
Glasgow, United Kingdom
james.windmill@strath.ac.uk

Dr Joseph Jackson
Centre for Ultrasonic Engineering
University of Strathclyde
Glasgow, United Kingdom
joseph.jackson@strath.ac.uk

Momchil Vasilev
Centre for Ultrasonic Engineering
University of Strathclyde
Glasgow, United Kingdom
momchil.vasilev@strath.ac.uk

***Abstract*— Acoustic metamaterials that operate on low frequency, in-air ultrasound have remained underdeveloped in spite of the numerous applications that utilise this bandwidth (e.g. distance ranging, air coupled ultrasonic testing) and instances where it is an unwelcome by-product (e.g. jet engines, PA systems). Here, the process of scaling a pre-existing acoustic beam shifter design – a structure that laterally shifts an incident wave – to operate in the 40 kHz bandwidth is detailed from numerical analysis, to finite element simulation, fabrication by additive manufacturing, and physical testing by sound pressure field mapping. The measured shift distance agreed well with the analytical and simulated results.**

Keywords—acoustic metamaterial, low frequency ultrasound, acoustic beam shifter, 3D printing

I. Introduction

Acoustic metamaterials have developed from an analogue of its electromagnetic predecessor to a burgeoning field with advances of its own [1–3]. Much attention has been given to the control of audible sound while in-air ultrasound applications have remained underdeveloped. Ultrasound from 18–50 kHz has been used in range-finders, acoustic spotlights, timber inspection, and acoustic levitation, and is a by-product of jet engines, PA systems and ultrasonic baths. Manipulation of sound in this frequency range has the potential to enhance transducer performance, simplify or surpass traditional solutions, and generate novel means of control.

Presented here is an acoustic beam shifter (ABS), as proposed by Wei [4], scaled to operate in the 40 kHz bandwidth. The ABS laterally shifts an incident wave and exhibits enhanced transmission at tuneable resonances. Development from analysis, to simulation, then fabrication and testing is detailed.

II. Context

A. An acoustic beam shifter design

The ABS is an array of plates with length l_{plate} and width w_{plate}, tilted at an angle θ and separated laterally by a distance p_{lat}, that create parallel channels through which an acoustic wave propagates. When the plates are tilted, l_{plate} is greater than the length of the channel that is bound on both sides $l_{bound} = l_{plate} - p_{lat} \sin\theta$. The effective acoustic length of the channel l_{eff} is approximately equal to the averaged length $l_{avg} = l_{plate} - (p_{lat} \sin\theta) / 2$. See Fig. 1 (Left).

Consider the ABS immersed in a background fluid (e.g. air). A wave propagating at an angle ϕ relative to the normal of the structure interface enters the channels, transverses the width of the ABS by undergoing multiple reflections from the plates and exits laterally shifted a distance $\Delta S = l_{eff} \sin(\phi + \theta)$ relative to its unimpeded position. See Fig. 1 (Right).

A plane wave has specific acoustic impedance $z_1 = \rho c / \cos\phi$ in the background medium and $z_2 = \rho c / (f \cos\phi)$ within the ABS channels, where ρ and c are the fluid's mass-density and acoustic wave speed and $f = 1 - w_{plate} / (p_{lat} \cos\theta)$ is the so called filling fraction – a measure of unoccupied space for a given area.

Consider the transmitting boundary of the ABS as a line of acoustic sources each of which has radius $a = p_{lat} / 2$; a directivity; and associated near and far fields. If two behaviours are demanded from these sources then radius a, and p_{lat}, can be appropriately constrained. First, the directivity index of each source should be negligible to preserve the profile of an input

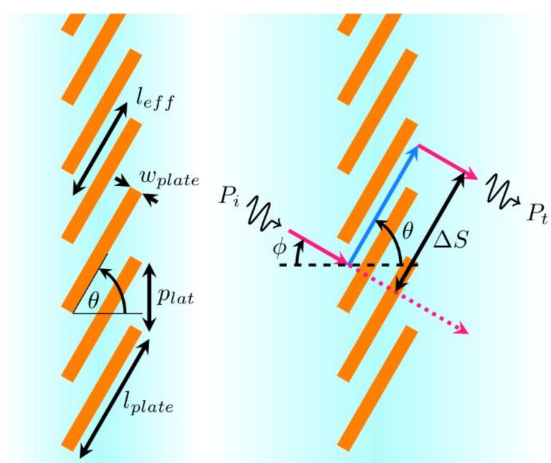

Fig. 1. **(Left)** The ABS with plate length, width, lateral separation and angle indicated by l_{plate}, w_{plate}, p_{lat} and θ. Effective acoustic length of the channels between the plates, l_{eff}, is also indicated. **(Right)** A pressure wave P_i incident on the structure at an angle ϕ propagates through the channels and is transmitted as P_t, laterally shifted a distance ΔS with respect to the reference, dotted beam.

This work received funding from the European Research Council under the European Union's Seventh Framework Programme FP/ 2007-2013/ERC grant no. 615030.

wave. Second, the near field's extent should be minimised and the far field established shortly.

The first demand is satisfied when the radius is less than one-sixth of a wavelength, or equivalently, $ka < 1$ [5] but determining the transitory point between near and far fields is not so simple [6]. If the near field distance $r_{nf} = 4a^2/\lambda$ – an established conservative measure [7] – then when the first demand is met and $a < \lambda/6$ then so also is the second and $r_{nf} = \lambda/9$. Hereafter it is assumed that $p_{lat} < \lambda/3$.

III. Methods

A. Numerical analysis

The amplitude transmission and reflection coefficients t and r for an acoustic wave that has propagated from a first medium, through a second with thickness l, into a third, where the impedance in each medium is z_1, z_2 and z_3, can be found in the literature [8]. If changes – $l \rightarrow l_{eff}$, $z_1 = z_3$ and $k_1 = k_2 = k_3 \rightarrow k$ – are made to the generalised case then, for the ABS configured as per Fig. 1:

$$t = 2/(2\cos kl_{eff} + \mathrm{j}\,(z_2/z_1 + z_1/z_2)\sin kl_{eff}) \quad (1)$$

$$r = \mathrm{j}\,d/(e + \mathrm{j}\,g) \quad (2)$$

where $d = (z_2/z_1 - z_1/z_2)\sin kl_{eff}$, $e = 2\cos kl_{eff}$, and $g = (z_2/z_1 + z_1/z_2)\sin kl_{eff}$. Consequently, the acoustic power transmission coefficient ($T = 1 - R$, where $R = |r|^2 = rr^*$ is the acoustic power reflection coefficient) is:

$$T = (e^4 + g^4 - d^2e^2 - d^2g^2 + 2\,e^2g^2)/(e^4 + g^4 + 2\,e^2g^2) \quad (3)$$

Transmission is maximised when $kl_{eff} = n\pi$ where n is a non-negative integer. Increasing z_2/z_1 causes a more discriminating response and so it is possible to transmit selected, harmonically related frequencies and attenuate others.

The quotient is dependent on ϕ, θ and f. However, here, only $\phi = 0°$ is considered and so (with reference to f) we are left with w_{plate}/p_{lat} and θ. However, changes in θ also affect ΔS. Therefore, in designing an ABS, a frequency of interest – one to be maximally transmitted – is chosen first, prescribing k and l_{eff}. A desired ΔS is chosen, setting θ, second. Finally, w_{plate}/p_{lat} is tuned for the required response (and $p_{lat} < \lambda/3$ if a negligible directive index is preferred). See the responses for different values of w_{plate}/p_{lat} in Fig. 2.

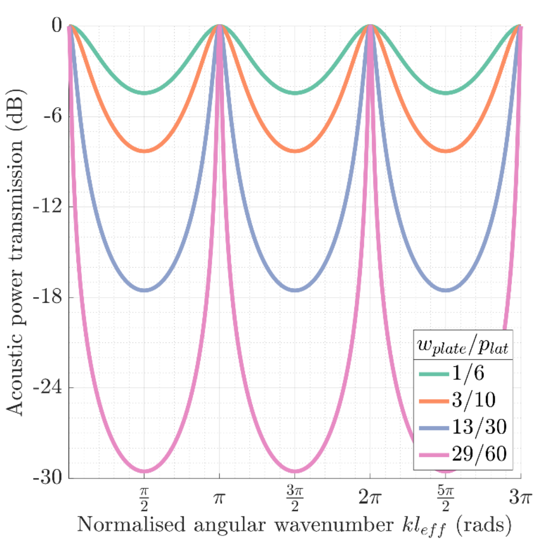

Fig. 2. The analytical acoustic power transmission response of an ABS for a normally incident wave. Plate angle $\theta = 60°$, and w_{plate}/p_{lat} ratios 1/6, 3/10, 13/30 and 29/60 generate ratios z_2/z_1 of 3, 5, 15 and 60.

B. Simulation

The Acoustics Module of COMSOL Multiphysics was used to simulate the effect of a number of different ABS designs on planar, time harmonic, waves. The design is demonstrably capable for a range of geometries but for the sake of brevity l_{plate} and θ will be held constant here at 10 mm and 60°. Unless stated otherwise, the "Pressure Acoustics, Frequency Domain" studies ran at 41 frequencies: 30 kHz to 50 kHz in 500 Hz increments.

1) A lateral beam shift

A reference model was made, then nineteen "Sound Hard Boundaries" (ABS plates with $p_{lat} = 2.5$ mm) were introduced. Compare the Sound Pressure Level (SPL) distribution of both configurations in Fig. 3 – a lateral shift is clearly visible. Absolute pressure data was exported from both models as a regular grid with 0.25 mm spacing and these arrays were cross-correlated (i.e. the reference beam was "found" in the shifted field) to quantify the shift.

Thermoviscous losses were accounted for by inclusion of a "Narrow Region Acoustics" "Rectangular duct" in the entirely bounded channel areas. Finally, the plates were considered as a solid with density 1180 kg m^{-3}, Young's modulus 1.6 GPa and Poisson's ratio 0.35 (values that are known to correspond well with the intended fabrication material) and "Solid Mechanics" and "Acoustic-Structure Boundaries" were included. Similarly, absolute pressure data was exported from these models and cross-correlated with the reference.

2) Acoustic power transmission response

The acoustic power transmission response through the structure was calculated by evaluating the integrals of acoustic intensity over the entrance and exit boundaries. For the ABS design detailed here transmission peaks were found at 40 550 Hz, 38 550 Hz and 38 820 Hz in the 'hard boundaries', 'with losses' and 'acoustic-structure with losses' models, respectively.

It was demonstrable that l_{eff} was proportional to p_{lat}. In addition, the analytical response predicted a transmission peak at 38 486 Hz, which was less than those suggested by the simulations. Subsequently, an acoustic end correction was calculated (but not presented here) to better predict the transmission peak for a given geometry.

C. Fabrication

The ABS design that was chosen to fabricate was composed of five rows of nineteen angled plates (with $l_{plate} = 10$ mm, $w_{plate} = 0.5$ mm, $p_{lat} = 2.5$ mm, $\theta = 60°$ and height 6 mm) stacked vertically and interspersed by four horizontal support plates (with length 53.91 mm, breadth 5.43 mm and height 0.6 mm). Corner columns (of length and breadth 2 mm and height 32.4 mm) pass through the support plates joining thicker, border buttresses (with height 4 mm).

It was fabricated with a commercial 3D stereolithographic printer (Asiga PICO2 HD) and resin (Formlabs Clear Resin, RS-F2-GPCL-04) then post-cured (Asiga Flash DR-301C).

D. Physical testing

The purpose of physical testing was to demonstrate and quantify the lateral shift of a sound field following propagation through the ABS.

An ultrasonic transducer (Ultra Sound Advice S55 Loudspeaker powered by S56 Amplifier) was centred over a 30 mm-by-30 mm square aperture that was cut into a steel baffle. The transducer transmitted a packet of 41 asynchronous sinusoidal signals that were output from a DAQ operating at 140 kHz (National Instruments USB-6251 and BNC-2201). The generated field propagated through the air channels of the ABS (or into the free field, as appropriate). A calibrated microphone (Brüel & Kjær Microphone Cartridge Type 4138 and Microphone Preamplifier Type 2670 in conjunction with Brüel & Kjær NEXUS Conditioning Amplifier Type 2692-A) fastened to a six degree of freedom robotic manipulator (KUKA KR6 R900 AGILUS) and input to the DAQ received the transmission. On completion of transmission and capture the robot moved the microphone to a new position and the processes was repeated. In total, measurements were made at 25 921 positions across a 40 mm-by-40 mm grid with 0.25 mm resolution. It moved to the same positions in instances with and without the ABS in place.

The microphone was positioned normal to the generated field. In the bandwidth studied here, the free field correction to the pressure response at 90° is less than 2 dB [10]. The correction was not applied as relative levels were of interest.

Robot automation was implemented in the LabVIEW programming environment and real time robot control was achieved through the KUKA Robot Sensor Interface and the in-house developed Interfacing Toolbox for Robot Arms [11].

Each signal packet was composed of 41 sinusoids, that increased from 30 kHz to 50 kHz in 500 Hz increments. Each discrete signal was 1 ms in duration and offset in time by 1 ms. During each offset period ambient noise was captured for use in post-capture SNR calculations. Additional samples were captured to account for time of flight between the transducer and the microphone at maximal range. Signal generation, transmission and capture were controlled by the LabVIEW programming environment.

E. Analysis

The spectra of each signal in the packet (and of the ambient noise captured directly before its transmission) was calculated, then the spectral amplitude level at the transmission frequency was extracted to produce 41 mono-frequency "pressure maps". The SPL difference between transmission and ambient noise pressure maps was at least 10 dB throughout. The reference pressure maps were cross-correlated with those that had the ABS in place to calculate ΔS. See Fig. 4.

IV. Results

Beam shift distance was calculated for each of the studies discussed and are presented in Table 1. As ΔS was calculated for each signal in the packet a median can be calculated: the negligible standard deviation suggests that ΔS is frequency invariant.

TABLE I. BEAM SHIFT DISTANCE

Study type		ΔS (mm)	Standard deviation
Analytical ($l_{eff} \approx l_{avg}$)		7.7	–
COMSOL Multiphysics simulation	Sound Hard Boundaries (median; n =41)	7.5	0.10
	Sound Hard Boundaries & Narrow Region Acoustics (median; n = 41)	7.5	0.10
	Acoustic Structure Boundary Multiphysics & Narrow Region Acoustics (median; n = 41)	7.3	0.28
Experimental (median; n = 41)		8.0	0.49

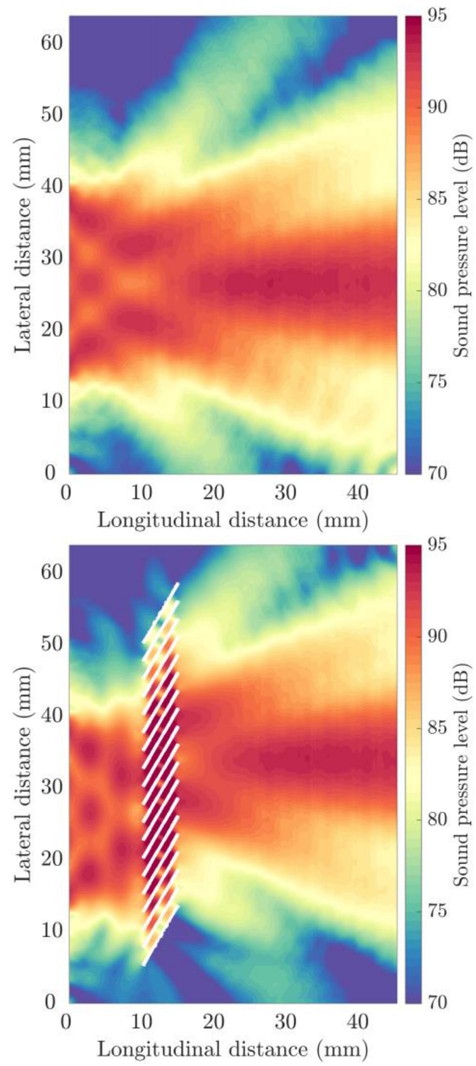

Fig. 3. SPL distribution of a 40 000 Hz, 1 Pa (≈ 94 dB) plane wave propagating from a "Background Pressure Field" in COMSOL. An SPL scale was used, and bound between 70 dB and 95 dB, for clarity. (**Top**) With no plates the wave propagates freely. (**Bottom**) The ABS laterally shifts the sound field upwards while largely retaining its planar profile.

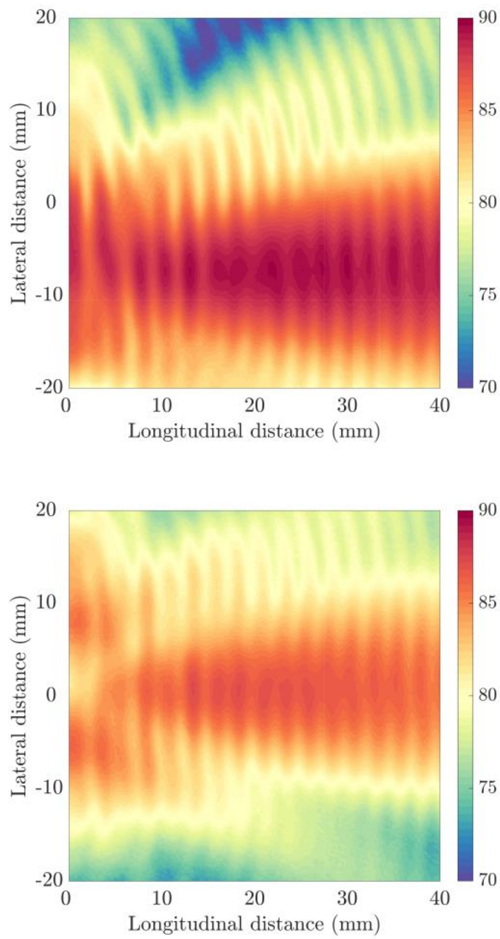

Fig. 4. An experimentally captured SPL distribution of a 40 000 Hz wave. As per the simulation **(Top)** the wave propagates freely with noABS in place and **(Bottom)** is laterally shifted upwards when it is.

V. Discussion

Analytical, simulated and experimental results agreed well. The experimental ΔS was 3.9% greater than the analytical result and between 6.7–9.6% greater than that predicted by the COMSOL simulation. While these differences are small, it could potentially be reduced by improvements to the experimental configuration such as increased grid resolution, longer signal transmission times and fitting of sound absorbing materials around the transducer and microphone to minimise interference from reflections.

VI. Conclusion

A pre-existing ABS design was scaled to operate in the low frequency, ultrasonic bandwidth. An analysis of its function was detailed; its effect on an incident plane wave was simulated; then it was fabricated, and physically tested. The beam shift distances calculated from each study type were found to be in good agreement. This design, rapidly realisable by additive manufacturing, that can laterally shift a sound field may prove useful in ultrasonic range finders or air coupled ultrasonic testing, in particular, when additional electronics or processing is expensive and undesirable.

In the immediate future a transmission response will be extracted from the dataset and compared to the analytical and simulated responses. The acoustic end correction will also be detailed. Later, the effect of varying the angle of incidence ϕ will be simulated and experimentally determined.

References

[1] S. A. Cummer, J. Christensen and A. Alù, “Controlling sound with acoustic metamaterials,” Nature Reviews Materials, vol. 1, no. 3, p. 16001, 2016.

[2] G. Ma and P. Sheng, “Acoustic metamaterials: From local resonances to broad horizons,” *Science Advances,* vol. 2, no. 2, p e1501595, 2016.

[3] D. Lee, D. M. Nguyen and J. Rho, “Acoustic wave science realized by metamaterials,” Nano Convergence, vol. 4, no. 1, p. 3, 2017.

[4] P. Wei, F. Liu, Z. Liang, Y. Xu, S. T. Chu and J. Li, “An acoustic beam shifter with enhanced transmission using perforated metamaterials,” *EPL,* vol. 109, p. 14004, 2015.

[5] L. L. Beranek, Acoustics, New York: Acoustical Society of America, 1993, pp. 91-95.

[6] K. G. Foote, “Discriminating between the nearfield and the farfield of acoustic transducers,” The Journal of the Acoustical Society of America, pp. 1511-1517, 2014.

[7] E. Skudrzyk, The Foundation of Acoustics: Basic Mathematics and Basic Acoustics, Wien: Springer, 1971, pp. 631-633.

[8] D. T. Blackstock, Fundamentals of physical acoustics, New York: Wiley & Sons Ltd, 2000, pp. 163-165.

[9] L. E. Kinsler, A. R. Frey, A. B. Coppens and J. V. Sanders, Fundamentals of acoustics, New York: John Wiley & Sons, 2000, p. 274.

[10] Brüel & Kjær, ″1/8″ Pressure-field Microphone - Type 4138,″ 12 September 2019. [Online]. Available: https://www.bksv.com/-/media/literature/Product-Data/bp2030.ashx. [Accessed 2019 September 2019].

[11] C. Mineo, M. Vasilev, C. N. MacLeod, R. Su, G. Pierce, C. Wong, E. Yang, R. Fuentes and E. J. Cross, “Enabling Robotic Adaptive Behaviour Capabilities for New Industry 4.0 Automated Quality Inspection Paradigms,” in 57th Annual British Conference on Non-Destructive Testing, Nottingham, 2018.